J. Fluid Mech. (2009), *vol.* 620, *pp.* 241–262.
doi:10.1017/S002211200800459X Printed in the United Kingdom

Macro-scale description of transient electro-kinetic phenomena over polarizable dielectric solids

G. YOSSIFON[1]†, I. FRANKEL[2] AND T. MILOH[1]‡

[1]School of Mechanical Engineering, University of Tel-Aviv, Tel-Aviv 69978, Israel

[2]Faculty of Aerospace Engineering, Technion-Israel Institute of Technology, Haifa 32000, Israel

(Received 11 February 2008 and in revised form 24 September 2008)

We have studied the temporal evolution of electro-kinetic flows in the vicinity of polarizable dielectric solids following the application of a 'weak' transient electric field. To obtain a macro-scale description in the limit of narrow electric double layers (EDLs), we have derived a pair of effective transient boundary conditions directly connecting the electric potentials across the EDL. Within the framework of the above assumptions, these conditions apply to a general transient electro-kinetic problem involving dielectric solids of arbitrary geometry and relative permittivity. Furthermore, the newly derived scheme is applicable to general transient and spatially non-uniform external fields. We examine the details of the physical mechanisms involved in the relaxation of the induced-charging process of the EDL adjacent to polarizable dielectric solids. It is thus established that the time scale characterizing the electrostatic relaxation increases with the dielectric constant of the solid from the Debye time (for the diffusion across the EDL) through the 'intermediate' scale (proportional to the product of the respective Debye- and geometric-length scales). Thus, the present rigorous analysis substantiates earlier results largely obtained by heuristic use of equivalent RC-circuit models. Furthermore, for typical values of ionic diffusivity and kinematic viscosity of the electrolyte solution, the latter time scale is comparable to the time scale of viscous relaxation in problems concerning microfluidic applications or micro-particle dynamics. The analysis is illustrated for spherical micro-particles. Explicit results are thus presented for the temporal evolution of electro-osmosis around a dielectric sphere immersed in unbounded electrolyte solution under the action of a suddenly applied uniform field, combining both induced charge and 'equilibrium' (fixed charge) contributions to the zeta potential. It is demonstrated that, owing to the time delay of the induced-EDL charging, the 'equilibrium' contribution to fluid motion (which is linear in the electric field) initially dominates the (quadratic) 'induced' contribution.

1. Introduction

When considering fluid motion on micro-scales, viscous relaxation is typically achieved within milliseconds. The time evolution of microflows is nevertheless highly

† Present address: Center for Microfluidics and Medical Diagnostics, Department of Chemical and Biomolecular Engineering, University of Notre Dame, Notre Dame IN 46556, USA.
‡ Email address for correspondence: miloh@eng.tau.ac.il

relevant to a growing variety of applications of electro-kinetics in microfluidics and colloidal dynamics in the sub-millisecond range. These include *inter alia* biochip operation in high-speed electrophoretic separation processes (Fan & Harrison 1994; Jacobson *et al.* 1994, 1998), the use of short-duration pulsed electric fields (Soderman & Jonsson 1996) in order to distinguish between particle velocities and background electro-osmotic flow or to suppress thermal-zone broadening (Dose & Guiochon 1993) as well as micro-mixing and micro-pumping by means of AC or modulated DC fields (Ramos *et al.* 1999; Ajdari 2000; Gonzalez *et al.* 2000; Brown, Smith & Rennie 2002). Owing to the short time scales involved, it is essential to account for the unsteady dynamics of the electro-kinetic flows in these applications.

Within the framework of the standard assumptions of 'narrow'-electric double layer (EDL) and weak electric fields (Lyklema 1995) the leading-order electrostatic and hydrodynamic problems are decoupled. The solution of the former yields the fluid slip velocity at the outer edge of the EDL. Furthermore, for EDL width h, typically of the order of a few tens of nm, viscous relaxation within the EDL is practically instantaneous ($h^2/\nu \approx 10^{-9}$ s where for aqueous solutions we take the kinematic viscosity $\nu \approx 10^{-2}\,\mathrm{cm^2\,s^{-1}}$). Hence (cf. Squires & Bazant 2004), incorporating the instantaneous local values of ζ and E_s, the dimensionless zeta potential and tangential component of the electric field, respectively, we may still (quasi-steadily) apply the familiar Helmholtz–Smoluchowski relation to obtain the dimensionless slip velocity

$$v_s = -\zeta E_s, \tag{1.1}$$

at all time $t > 0$. In (1.1) v_s, E_s and ζ are respectively normalized by $\varepsilon_0 \varepsilon_f E_0 \phi_0/\eta$, E_0 and $\phi_0 = E_0 \varepsilon_w h\, a/(\varepsilon_f a + \varepsilon_w h)$ (cf. Murtsovkin 1996; Yossifon, Frankel & Miloh 2007), where ε_0 is the electric permittivity of vacuum, ε_f and ε_w denote the dielectric constants of the electrolyte solution and solid wall, respectively, E_0 is a characteristic magnitude of the external field, η is the dynamic fluid viscosity and a is a geometric length scale of the problem.

Most previous analyses of transient electro-kinetic phenomena have focused on non-polarizable solids. They have accordingly assumed constant (instantaneously established) slip velocity and (uniform) zeta potential and thereby studied transient electrophoresis (Morrison 1969, 1971; Ivory 1984; Keh & Huang 2005) and electro-osmosis (Hanna & Osterle 1968; Ivory 1983; Soderman & Jonsson 1996; Keh & Tseng 2001; Santiago 2001; Kang, Yang & Huang 2002; Yang, Ng & Chan 2002; Erickson & Li 2003; Luo 2004; Yang *et al.* 2004; Campisi, Accoto & Dario 2005; Mishchuk & Gonzalez 2006; Zhang *et al.* 2006) in response to various modes of suddenly applied external fields.

In the presence of polarizable solids the external field (presumed weak) does, however, affect the diffuse charge within the (thin) EDL. This interaction is manifested in a zeta potential which is no longer an equilibrium material property, but rather depends upon the applied field. These induced-charge effects have been extensively studied in polarizable colloidal particles (Levich 1962; Simonov & Dukhin 1973; Simonov & Shilov 1973; Dukhin & Murtsovkin 1986, see also Squires & Bazant 2004 and references cited therein) and more recently in the context of microfluidic applications (e.g. Ramos *et al.* 1999; Ajdari 2000; Gonzalez *et al.* 2000; Brown *et al.* 2002; Bazant & Squires 2004; Harnett *et al.* 2008) largely under steady or AC fields.

While most attention has focused on electro-kinetics in the vicinity of conductors, it is well known that the very (often inevitable) presence of a thin dielectric layer of surface contamination (for instance by oxides or adsorbed species on electrode

surfaces) can substantially modify the induced zeta potential and the associated electro-kinetic phenomena. The significance of polarization effects has also been established for the dynamics of spherical (Dukhin 1986; Gamayunov, Murtsovkin & Dukhin, 1986; Murtsovkin 1996; Miloh 2008*a*) and non-spherical (Yossifon *et al.* 2007; Miloh 2008*b*; Yariv 2008) colloidal dielectric particles as well as for the flows around corners at junctions of nearly insulating micro-channels (Thamida & Chang 2002; Takhistov, Duginova & Chang 2003; Yossifon, Frankel & Miloh 2006) and in microfluidic mixing applications (Nadal *et al.* 2002; Wang *et al.* 2006).

An important aspect of the transient induced-charge electro-kinetic problem is the relaxation time scale of the electrostatic problem which (Macdonald 1970) may reach here the 'intermediate' scale ha/D (where D denotes an ionic diffusion coefficient). For typical values ($D \approx 10^{-5}\,\mathrm{cm^2\,s^{-1}}$, $\delta = h/a \approx 10^{-3}$), we have $ha/D \sim a^2/\nu$, *i.e.* both electrostatic and hydrodynamic relaxation processes may take place on comparable time scales. Evidently, unlike the above-mentioned examples of non-polarizable solids, one cannot assume here an instantaneously established (step function) fluid slip velocity.

The study of transient induced-charge electro-kinetic problems has so far considered only the dynamics of the diffuse electric charge (as opposed to the complete electro-kinetic problem including the temporal evolution of the attendant fluid motion). Furthermore, previous analyses of the relaxation process in the electrostatic problem have essentially been confined to simple geometrical configurations (e.g. planar electrodes, spherical colloidal particles) of *conducting* solids (Bazant, Thornton & Ajdari 2004; Chu & Bazant 2006). Existing estimates of the relaxation time scale for polarizable dielectric solids are largely based on the use of heuristic equivalent electric-circuit models.

The aim of the present contribution is thus to gain a better understanding of the physical processes underlying the transient electro-kinetic relaxation phenomena following the application of an external field in the presence of polarizable solids (of arbitrary shape and dielectric permittivity). Owing to the large-scale disparity associated with the narrow-EDL problem, we seek to obtain, in a similar manner to corresponding steady electro-kinetic problems, a macro-scale description avoiding the need to resolve the details of the EDL. To this end we derive in the next section effective leading-order boundary conditions directly relating the electric potentials within the bulk electroneutral solution and the solid wall, respectively. The actual analysis needs only to address the transient electrostatic problem for uncharged polarizable solids. However, this subsequently affects the time evolution of the electro-osmotic flows associated with the respective contributions of both the induced and equilibrium surface charge. The newly derived conditions are general in the sense that they apply to arbitrary external-field variation, solid geometry (provided that $\delta \ll 1$ is uniformly satisfied) and material (dielectric) properties. They are subsequently applied in § 3 to analytically study the time evolution of electro-osmosis around a dielectric sphere immersed in a symmetric electrolyte solution of equal ionic diffusivities following the application of a general non-uniform axisymmetric electric field. Explicit results are then presented for a suddenly applied uniform field. By means of these we can quantitatively examine the effects of the solid dielectric constant and the relative magnitudes of the respective 'induced' and 'equilibrium' parts of the zeta potential on the evolution of the resulting flow. Further discussion and concluding comments appear in § 4. The Appendices outline the calculation of the stream function (Appendix A) and inverse Laplace transforms (Appendix B), respectively.

2. Effective macro-scale boundary conditions in the transient electrostatic problem

We consider a symmetric electrolyte ($z^+ = -z^- = z$) and make the standard assumptions of a thin EDL (i.e. $\delta \ll 1$) and weak electric fields (i.e. $\Psi = z F\phi_0/\Re\Theta \ll 1$, cf. Lyklema 1995), wherein F denotes the Faraday number, $\Re$ the universal gas constant and Θ the absolute temperature. Within this framework, the hydrodynamic and electrostatic problems are decoupled. Furthermore, the domain of the latter problem separates into three sub-domains: the electroneutral solid wall and bulk solution with their harmonic electric potentials φ_w and φ_f, respectively, and the 'inner' domain of the diffuse EDL whose electric potential ϕ satisfies Poisson's equation. To obtain the requisite macro-scale conditions connecting φ_w and φ_f on the solid–electrolyte interface, we focus on the inner domain which (for $\delta \ll 1$) is locally one-dimensional in the direction of the coordinate line y' normal (in the outward sense) to the surface of the solid. We define the corresponding 'outer' (y) and 'inner' (Y) dimensionless variables through

$$y' = ay = hY. \tag{2.1}$$

In the present approximation, the concentrations of the ionic species normalized by n_0, the uniform ambient concentration of the bulk solution, can be described by

$$n_i = 1 + 2\Psi\,\hat{n}_i \quad (i = 1, 2), \tag{2.2}$$

where $\hat{n}_i$ denote deviations of the (dimensionless) local concentrations of anions and cations ($i = 1$, 2, respectively) from the uniform bulk concentration. To leading order (in the limit of small δ and Ψ) ϕ and $\hat{n}_i (i = 1, 2)$ satisfy the approximate forms of both Poisson's equation

$$\frac{\partial^2\phi}{\partial Y^2} = -(\hat{n}_1 - \hat{n}_2), \tag{2.3}$$

and the continuity (Nernst–Planck) equations for the ionic species

$$\beta_i^2 \frac{\partial \hat{n}_i}{\partial t} = \frac{\partial^2 \hat{n}_i}{\partial Y^2} \mp \frac{1}{2}(\hat{n}_1 - \hat{n}_2) \quad (i = 1, 2). \tag{2.4}$$

In (2.4) $\beta_i^2 = h^2/D_i T$, wherein T is the appropriate time scale (to be specified later on) and D_i ($i = 1, 2$) denote the respective ionic diffusivities of the solute. On the surface of the solid ϕ and $\hat{n}_i$ satisfy the electrostatic conditions

$$\phi = \varphi_w \quad \text{and} \quad \frac{\partial\phi}{\partial Y} - \alpha\frac{\partial\varphi_w}{\partial y} = -\sigma \quad \text{at } y, Y = 0, \tag{2.5a, b}$$

and the vanishing of the normal components of the respective ionic fluxes, i.e.

$$\frac{\partial \hat{n}_i}{\partial Y} = \mp\frac{1}{2}\frac{\partial\phi}{\partial Y} \quad (i = 1, 2) \quad \text{at } Y = 0. \tag{2.6}$$

In (2.5b) $\alpha = (\varepsilon_w/\varepsilon_f)\delta$ and σ is the dimensionless equilibrium (i.e. independent of any externally applied field) surface charge density which is scaled by $\phi_0\varepsilon_0\varepsilon_f/h$ and presumed uniform over the solid surface. At the outer edge of the EDL we impose the asymptotic matching condition

$$\phi|_{Y\to\infty} \sim \varphi_f|_{y\to 0}, \tag{2.7}$$

and the electroneutrality condition

$$\hat{n}_i = 0 \quad (i = 1, 2) \quad \text{as } Y \to \infty. \tag{2.8}$$

The above equations and boundary conditions are supplemented by the initial conditions

$$\hat{n}_i(Y,0) = \hat{n}^{(eq)}(Y) \quad (i = 1, 2). \tag{2.9}$$

The linearity of the present problem allows for the generic representation $f = f^{(in)} + f^{(eq)}$ of ϕ and $\hat{n}_i$ as a superposition of an 'equilibrium' part (eq) exclusively associated with σ and an 'induced' part (in) satisfying the above problem with (2.5b) and (2.9) replaced by their homogeneous counterparts. In the sequel we focus on the 'induced' part of the problem. To simplify the notation we accordingly omit the superscript (in) unless it simultaneously appears together with (eq).

We generically denote by $G(Y,s)$ the Laplace transform of $g(Y,t)$

$$G(Y,s) = \int_0^\infty \mathrm{e}^{-st} g(Y,t)\,\mathrm{d}t = L\{g(Y,t)\}. \tag{2.10}$$

The transformed problem resulting from (2.4), (2.6) and (2.8) together with the homogeneous initial conditions readily yields $N_i(Y,s) = L\{\hat{n}_i(Y,t)\}$ $(i = 1,\ 2)$. Substituting these into the right-hand side of the transformed (2.3) and integrating twice with respect to Y, while denoting by $(F_f, F_w, F) = \int_0^\infty \mathrm{e}^{-st}(\varphi_f, \varphi_w, \phi)\,\mathrm{d}t$ the Laplace transform of the various potentials, we obtain

$$F(Y,s) = \left(\frac{\partial F}{\partial Y}\right)\bigg|_{(0,s)} \left[\left(1 + \frac{B_1(s)}{\lambda_1^2} + \frac{B_2(s)}{\lambda_2^2}\right) Y + \frac{B_1(s)}{\lambda_1^3}\mathrm{e}^{-\lambda_1 Y} + \frac{B_2(s)}{\lambda_2^3}\mathrm{e}^{-\lambda_2 Y}\right] + A(s), \tag{2.11}$$

where

$$\lambda_{1,2}^2 = \tfrac{1}{2}\left[1 + \left(\beta_1^2 + \beta_2^2\right)s \pm \sqrt{1 + \left(\beta_1^2 - \beta_2^2\right)^2 s^2}\right]. \tag{2.12}$$

In (2.11) we select for $\lambda_{1,2}$ those branches where $\lambda_{1,2} > 0$ for $s > 0$; the explicit expressions of $B_{1,2}(s;\beta_1,\beta_2)$ are here omitted. Applying the transformed matching condition (2.7) one gets

$$F_f \sim A(s) \quad \text{and} \quad \frac{\partial F_f}{\partial y} \sim \left(\frac{\partial F}{\partial Y}\right)\bigg|_{(0,s)} \frac{1}{\delta}\left(1 + \frac{B_1(s)}{\lambda_1^2} + \frac{B_2(s)}{\lambda_2^2}\right) \quad \text{as} \quad y \to 0.$$

Making use of these expressions we eliminate $A(s)$ and $(\partial F/\partial Y)|_{(0,s)}$ from the transformed conditions (2.5a, b) thereby obtaining

$$F_w - \alpha\left(\frac{B_1(s)}{\lambda_1^3} + \frac{B_2(s)}{\lambda_2^3}\right)\frac{\partial F_w}{\partial y} = F_f \quad \text{at } y = 0 \tag{2.13}$$

and

$$\frac{\partial F_f}{\partial y} = \frac{\alpha}{\delta}\left(1 + \frac{B_1(s)}{\lambda_1^2} + \frac{B_2(s)}{\lambda_2^2}\right)\frac{\partial F_w}{\partial y} \quad \text{at } y = 0. \tag{2.14}$$

Equations (2.13) and (2.14) constitute the Laplace-transformed version of the sought macro-scale transient conditions directly connecting F_w and F_f across the EDL. These effective newly derived conditions are a central result of the present analysis. They are applicable to the calculation of the transient induced-charge electro-kinetic flow around polarizable solids of any dielectric constant for a general geometry of the solid and an arbitrary time variation of the non-uniform external electric field. As such they present a rigorous alternative to the prevalent use of equivalent RC-circuit models. For all finite values of α, the solution of the transient macroscopic electrostatic problem thus consists of the simultaneous calculation of the potentials $\varphi_f(\boldsymbol{r},t)$ and $\varphi_w(\boldsymbol{r},t)$ (wherein $\boldsymbol{r}$ denotes the position vector) which are harmonic within

the respective electroneutral fluid and solid domains and satisfy (inverse transforms of) (2.13) and (2.14) on the surface of the solid (as well as the appropriate regularity and far-field conditions).

The subsequent derivation is considerably simplified when assuming equal ionic diffusivities. While $D_{1,2}$ are never strictly equal to each other (the closest case is, perhaps, potassium chloride wherein the respective ionic mobilities of the K^+ and Cl^- ions differ by some 4 %, see Lide 1994), this inequality is only of secondary importance with regard to our present purpose to gain physical insight into the relaxation process. By following the common practice (Gonzalez *et al.* 2000; Bazant *et al.* 2004; Squires & Bazant 2004) and assuming that $D_{1,2}=D$, $\beta_{1,2}=\beta$, $\lambda_1^2=1+\beta^2 s=\lambda^2$, $\lambda_2^2=\beta^2 s$, $B_1=-1$ and $B_2=0$. Thus, (2.13) and (2.14), respectively, simplify to

$$F_w+\frac{\alpha}{\lambda^3}\frac{\partial F_w}{\partial y}=F_f \quad \text{at} \quad y=0 \tag{2.15}$$

and

$$\frac{\partial F_f}{\partial y}=\frac{\alpha}{\delta}\frac{\beta^2 s}{\lambda^2}\frac{\partial F_w}{\partial y} \quad \text{at } y=0. \tag{2.16}$$

Taking inverse transformations of the above yield

$$\varphi_w+\frac{2\alpha}{\beta^3}\int_0^t\left(\frac{\partial\varphi_w}{\partial y}\right)\Big|_{(0,\tau)}\mathrm{e}^{-t-\tau/\beta^2}\left(\frac{t-\tau}{\pi}\right)^{1/2}\mathrm{d}\tau=\varphi_f \quad \text{at } y=0 \tag{2.15$'$}$$

and

$$\frac{\partial\varphi_f}{\partial y}=\frac{\alpha}{\delta}\left[\frac{\partial\varphi_w}{\partial y}-\frac{1}{\beta^2}\int_0^t\left(\frac{\partial\varphi_w}{\partial y}\right)\Big|_{(0,\tau)}\mathrm{e}^{-(t-\tau)/\beta^2}\,\mathrm{d}\tau\right] \quad \text{at } y=0, \tag{2.16$'$}$$

respectively, which constitute the key result of this section. In the small-time limit, i.e. $t\to 0^+$, (2.15′) and (2.16′) become equivalent to the homogeneous counterparts of (2.5) when replacing ϕ by φ_f, which is consistent with the initial (at $t=0^+$) absence of an induced EDL. In the other (long-time) limit, asymptotic expansions of the convolution integrals in (2.15′) and (2.16′) for small β^2 verify that they respectively reduce to the Robin-type and homogeneous Neumann conditions of the steady macro-scale electrostatic problem (Yossifon *et al.* 2007).

To gain some further physical insight into the relaxation process, we eliminate $\alpha\partial F_w/\partial y$ between (2.15) and (2.16) to obtain

$$\frac{1}{\lambda}\frac{\partial F_f}{\partial y}=\frac{\beta^2 s}{\delta}(F_f-F_w) \quad \text{at } y=0. \tag{2.17}$$

Taking the inverse transform in conjunction with the initial vanishing of $\zeta^{(in)}$, we get the time – evolution equation

$$\frac{1}{\pi^{1/2}\beta}\int_0^t\left(\frac{\partial\varphi_f}{\partial y}\right)\Big|_{(0,t-\tau)}\frac{\mathrm{e}^{-\tau/\beta^2}}{\tau^{1/2}}\,\mathrm{d}\tau=\frac{\beta^2}{\delta}\frac{\mathrm{d}}{\mathrm{d}t}(\varphi_f-\varphi_w) \quad \text{at } y=0. \tag{2.17$'$}$$

To leading order in $\beta^2\ll 1$ (i.e. $T\gg h^2/D$) the left-hand side of (2.17′) simplifies to yield the approximate charging equation

$$\frac{\partial\varphi_f}{\partial y}\sim\frac{\beta^2}{\delta}\frac{\mathrm{d}}{\mathrm{d}t}(\varphi_f-\varphi_w) \quad \text{at } y=0. \tag{2.17$''$}$$

Here the left-hand side represents the instantaneous Ohmic charging rate at the outer

edge of the EDL, which is equal to the growth rate of its total induced charge (or, equivalently, of $\zeta^{(in)}$) on the right-hand side. Appearing in (2.17) is the parameter β^2/δ representing the ratio of the two time scales ha/D and T. Also appearing in the above conditions is the parameter α which, in the terminology of an equivalent RC-circuit model, represents the ratio of the capacitance of the dielectric solid $\sim \varepsilon_w/a$ and that of the EDL $\sim \varepsilon_f/h$. From this analogy it is anticipated (cf. Bazant *et al.* 2004) that, when $\alpha \geqslant 1$, the difference $\varphi_f - \varphi_w$, effectively representing the induced zeta potential, becomes of comparable magnitude as φ_f. Consistent dominant balance in (2.17″) then requires that $\beta^2/\delta \sim O(1)$, thus suggesting that, for $\alpha \gtrsim 1$, the appropriate time scale of description is indeed the intermediate scale $T \sim ha/D$ (we return to this point in the next section, see (3.18) *et seq.*). In the limit $\alpha \to \infty$ (i.e. a conducting solid) $\varphi_w = 0$ and our result then precisely reduces to the macro-scale model of Squires & Bazant (2004, see their (7.48) and (7.50)).

Before proceeding to illustrate the use of the above general transient macro-scale conditions, we pause to consider the evolution of the charge-density distribution $c(Y,t) = \hat{n}_1 - \hat{n}_2$ (normalized by $\varepsilon_0 \varepsilon_f \phi_0/h^2$). By use of the above-mentioned Laplace transforms $N_{1,2}(Y,s)$, together with (2.5*b*) and (2.16) we obtain the transformed charge-density distribution. Inverse transformation and integration by parts then yield for equal ionic diffusivities

$$c(Y,t) = \delta \int_0^t \frac{\mathrm{d}\tau}{(\pi\tau)^{1/2}\beta} \mathrm{e}^{-[(\beta Y)^2/(4\tau)+\tau/\beta^2]} \left[\left(\frac{\partial \phi_f}{\partial y} \right)\Big|_{(0,t-\tau)} + \frac{1}{\beta^2} \int_0^{t-\tau} \left(\frac{\partial \phi_f}{\partial y} \right)\Big|_{(0,\tau_1)} \mathrm{d}\tau_1 \right]. \tag{2.18}$$

The instantaneous charge distribution within the EDL thus depends on the 'history' of both the rate of Ohmic charging and the time evolution of the total EDL charge represented by the first and second terms within the brackets in (2.18), respectively. This history dependence reflects time delays inherent in the charge redistribution processes within the EDL. Asymptotic expansion of (2.18) for $\beta^2 \ll 1$ while neglecting exponentially-small terms, leads to the rather simple expression for the transient charge-density distribution within the EDL

$$c(Y,t) \sim \frac{\delta}{\beta^2} \mathrm{e}^{-Y} \int_0^t \left(\frac{\partial \phi_f}{\partial y} \right)\Big|_{(0,\tau)} \mathrm{d}\tau + O(\delta). \tag{2.18′}$$

Before concluding this section and for future reference we note that when $T \gg h^2/D$ the charge distribution within the EDL has relaxed to a (quasi-) steady Boltzmann distribution normalized by the instantaneous total charge.

3. Transient ICEO past a dielectric sphere

The use of the effective boundary conditions derived above will now be demonstrated by applying them towards the macro-scale description of the electro-osmotic flow around a dielectric sphere. To avoid excessively tedious calculations we consider here the axisymmetric problem. For the externally applied electric potential

$$\varphi_a = \sum_{n=0}^{\infty} a_n(t) R^n P_n(\mu), \tag{3.1}$$

where (R, θ) are spherical polar coordinates and $P_n(\mu)\,(n=1, 2, \ldots)$ are the Legendre polynomials of $\mu = \cos\theta$, we express the electric potentials

$$\varphi_f = \varphi_a + \sum_{n=0}^{\infty} b_n(t)\, R^{-(n+1)} P_n(\mu) \quad \text{and} \quad \varphi_w = \sum_{n=0}^{\infty} c_n(t)\, R^n P_n(\mu). \tag{3.2,3.3}$$

Here, $b_n(t)$ and $c_n(t)$ denote time-dependent coefficients to be determined in terms of the prescribed coefficients of the applied field $a_n(t)$. Both φ_f and φ_w thus assumed are axisymmetric harmonic functions. The former satisfies the far-field condition $\varphi_f = \varphi_a$ when $R \to \infty$ and the latter is regular within the solid. We denote by $A_n(s)$, $B_n(s)$ and $C_n(s)$ the Laplace transforms of $a_n(t)$, $b_n(t)$ and $c_n(t)$, respectively. Applying then (2.15) and (2.16) at $R=1$, while identifying the local normal coordinate with R and making use of the orthogonality properties of the Legendre polynomials one gets

$$C_n(s) = \frac{(2n+1)\lambda^3}{(n+1+n(\alpha/\delta))\lambda^3 - n(\alpha/\delta)\lambda + n(n+1)\alpha} A_n(s), \tag{3.4}$$

where $\lambda(s)$ denotes the appropriate branch of $\lambda_1 = (1+\beta^2 s)^{1/2}$ (see (2.15)).

Next, $\zeta^{(in)}$, the induced zeta potential and E_s, the tangential component of the electric field at the surface of the sphere are expressed

$$\zeta^{(in)}(\theta, t) = -\sum_{n=1}^{\infty} z_n(t) P_n(\mu), \tag{3.5}$$

where the summation extends from $n = 1$ since $\zeta^{(in)}$ must integrate to zero over the sphere surface and

$$E_s(\theta, t) = \sum_{n=1}^{\infty} e_n(t)\, \dot{P}_n(\mu) \sin\theta, \tag{3.6}$$

respectively, wherein

$$z_n(t) = L^{-1}\left\{\frac{n\alpha}{\lambda^3} C_n(s)\right\},\ e_n(t) = L^{-1}\left\{\left(1 + \frac{n\alpha}{\lambda^3}\right) C_n(s)\right\}, \tag{3.7a, b}$$

and $\dot{P}_n(\mu)$ denotes $\mathrm{d}P_n(\mu)/\mathrm{d}\mu$. Using the quasi-steady *Helmholtz–Smoluchowski* relation (1.1), we then obtain the fluid slip velocity as the sum

$$v_s(\theta, t) = v_s^{(in)}(\theta, t) + v_s^{(eq)}(\theta, t), \tag{3.8}$$

of the respective induced

$$v_s^{(in)} = \sum_{m,n} e_m(t)\, z_n(t)\, P_n(\mu)\, \dot{P}_m(\mu)\, \sin\theta, \tag{3.9a}$$

and equilibrium

$$v_s^{(eq)} = -\zeta^{(eq)} \sum_{n} e_n(t)\, \dot{P}_n(\mu)\, \sin\theta, \tag{3.9b}$$

contributions. In (3.9*b*) $\zeta^{(eq)}$ is the dimensionless (normalized by ϕ_0) equilibrium zeta potential associated with the presumed uniform fixed surface-charge density σ (see (2.5*b*)). Evidently, $v_s^{(in)}$ and $v_s^{(eq)}$ differ from each other both in their distribution over the surface of the sphere as well as in their time evolution. Furthermore, it is worthwhile to note that unless $\alpha \ll 1$, the equilibrium contribution is affected by the 'induced' portion of the electrostatic problem through the relaxation process of

the tangential component of the electric field at the surface of the sphere (see the discussion of figure 1).

Once $v_s(\theta, t)$ has been obtained from the above solution of the electrostatic problem, we may next formulate the hydrodynamic problem. The unsteady creeping flow of the bulk electroneutral fluid is governed by the dimensionless continuity and Stokes equations,

$$div\, \boldsymbol{u} = 0 \quad \text{and} \quad \partial \boldsymbol{u}/\partial t + \nabla p = \nabla^2 \boldsymbol{u}, \tag{3.10, 3.11}$$

respectively, which are supplemented by the boundary slip velocity condition

$$\boldsymbol{u} = \boldsymbol{e}_\theta\, v_s(\theta, t) \quad \text{at} \quad R = 1, \tag{3.12}$$

the far-field attenuation condition

$$\boldsymbol{u} = 0 \quad \text{as} \quad R \to \infty, \tag{3.13}$$

and the initial condition $\boldsymbol{u} = 0$ at $t = 0$ for all $R \geqslant 1$, where $\boldsymbol{u}$ represents the fluid velocity vector. The pressure within the fluid p, and the time variable t, are here normalized by $\varepsilon_0 \varepsilon_f E_0(\phi_0/a)$ and a^2/ν, respectively.

It is convenient to make use of the axial symmetry of the present hydrodynamic problem and express the radial (u) and azimuthal (v) velocity components in terms of the Stokes stream function ψ

$$u = \frac{1}{R^2 \sin\theta}\frac{\partial \psi}{\partial \theta} \quad \text{and} \quad v = -\frac{1}{R \sin\theta}\frac{\partial \psi}{\partial R}. \tag{3.14a, b}$$

Substituting these in (3.11) leads to

$$E^2 \left(E^2 - \frac{\partial}{\partial t} \right) \psi = 0, \tag{3.15a}$$

where the operator E^2 expressed in spherical polar coordinates is (Happel & Brenner 1965)

$$E^2 = \frac{\partial^2}{\partial R^2} + \frac{\sin\theta}{R^2}\frac{\partial}{\partial \theta}\left(\frac{1}{\sin\theta}\frac{\partial}{\partial \theta} \right). \tag{3.15b}$$

These are supplemented by the boundary conditions

$$\psi = 0 \quad \text{and} \quad \frac{\partial \psi}{\partial R} = -v_s(\theta, t) \sin\theta \quad \text{at} \quad R = 1, \tag{3.16a, b}$$

as well as the far-field attenuation and the initial vanishing of the fluid velocity. The calculation of ψ for the general axisymmetric problem is outlined in Appendix A. Explicit results will now be presented for the common case of a uniform step-function external field.

3.1. *An illustration: A suddenly applied uniform field*

3.1.1. *The relaxation process of the electrostatic problem*

In this case the time variation of the external field is represented by Heavisides's function $H(t)$, hence the only non-vanishing coefficient in (3.1) is $a_1 = H(t)$. Accordingly $A_1(s) = -(E_0 a/\phi_0)/s$ (the multiplication factor is introduced so as to make the magnitude of the dimensionless external field equal to unity) and from (3.4)

$$C_1(s) = -\left(\frac{E_0 a}{\phi_0} \right) \frac{3}{s} \frac{\lambda^3}{(2 + \alpha/\delta)\lambda^3 - (\alpha/\delta)\lambda + 2\alpha}, \tag{3.17}$$

which is inverted in Appendix B to yield $c_1(t) = L^{-1}\{C_1(s)\}$ (B.5). From (B.5) we see that the relaxation process of the electrostatic problem is characterized by

both continuous and discrete eigenvalue spectra. The former, represented by the integral term in (B.5), reflects the simultaneous occurrence of both diffusive charge redistribution across the EDL and Ohmic charging. Since the diffusive transport across the EDL of the charge introduced at its outer edge takes place on the Debye (h^2/D) time scale, the instantaneous charge distribution $c(Y,t)$ depends not only upon the instantaneous values of the charging rate and total charge but rather on their entire time evolution from $t = 0^+$ (which has been anticipated in (2.18)). The dominant discrete eigenvalue of $c_1(t)$ occurs at

$$s_2 \sim -\frac{2\delta}{\beta^2}\left[\frac{1}{\alpha+2\delta}+\left(\frac{\alpha}{\alpha+2\delta}\right)^{1/2}\right], \tag{3.18}$$

to which corresponds the time scale

$$T \sim \frac{ha}{2D}\left[\frac{1}{\alpha+2\delta}+\left(\frac{\alpha}{\alpha+2\delta}\right)^{1/2}\right]^{-1}. \tag{3.19}$$

To estimate T we first note that for $\alpha \ll 1$ the expression in the square brackets is dominated by the first term. For $\alpha \sim 1$ both terms are comparable and the last term becomes dominant for $\alpha \gg 1$. From this we readily find that $T \sim O(h^2/D)$ for $\alpha \sim O(\delta)$, i.e. the relaxation process is controlled by diffusion across the EDL. For $\alpha \gg \delta$

$$T \sim \frac{ha}{2D}\frac{\alpha}{1+\alpha}. \tag{3.19$'$}$$

This expression is equivalent to leading order in $\delta \to 0$ to the result of Bazant *et al.* (2004, their (46)). Similar results have been obtained by Dukhin (1986), Ajdari (2000) and Squires & Bazant (2004) who sought to account for the effect on the relaxation time of the presence of a compact (Stern) layer or a dielectric coating within the framework of an equivalent RC-circuit model. Thus, the relaxation process is effectively represented by the charging of an equivalent capacitor (incorporating both the EDL and the dielectric solid) through an Ohmic bulk resistor (whose properties are determined by the combination of bulk ionic conductivity and length scale, respectively). As we have noted above (cf. (2.17$''$) *et seq.*), α represents the ratio of the capacitance of the dielectric solid to that of the EDL. The appearance of the multiplication factor $\alpha/(1+\alpha)$ in (3.19$'$) is indeed tantamount to the replacement of the capacitance of the EDL implicit in the intermediate time scale ha/D by the equivalent capacitance of the EDL and dielectric solid in a series combination. This equivalent capacitance and hence the corresponding relaxation time are both increasing with α, T approaching the upper limit $ha/2D$ when $\alpha \to \infty$ (for a conducting sphere). The present rigorous analysis thus substantiates the above-mentioned estimates of the appropriate relaxation time scale based on the use of modified RC models and demonstrates that, for $\alpha \gg \delta$, the relaxation process is indeed dominated by the Ohmic charging. Finally, we note that in the limit $\alpha \to \infty$, one obtains from (3.1), (3.2) and (B.6)

$$\varphi_f \sim -R\cos\theta\left[1+\frac{1}{2R^3}\left(1-3\mathrm{e}^{-(2\delta/\beta^2)t}\right)\right] \tag{3.19$''$}$$

in complete agreement with the result for a conducting sphere appearing in Table I of Squires & Bazant 2004.

Once the original function $c_1(t)$ has been determined, one can readily obtain from (3.5) and (3.6) the following expressions for the time evolution of both the induced

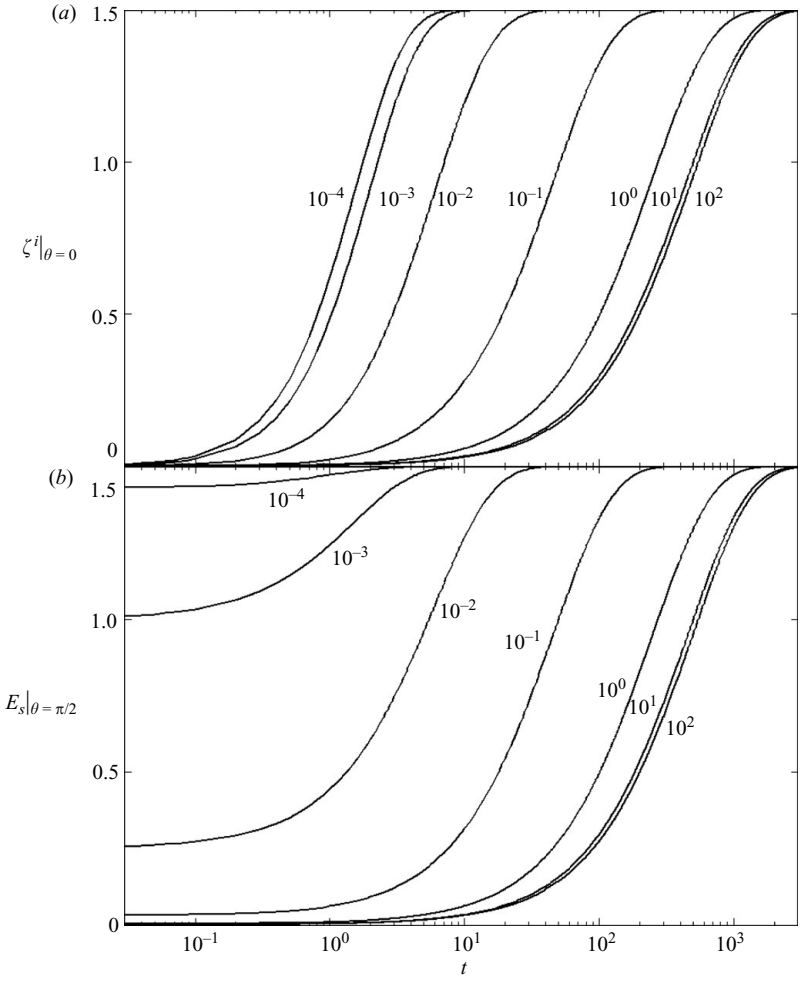

FIGURE 1. The effect of α on the evolution of the amplitude of the: (*a*) induced zeta potential; (*b*) tangential component of the electric field.

zeta potential

$$\zeta^{(in)}(\theta, t) = -\frac{2\alpha}{\beta^3}\left(\frac{t}{\pi}\right)^{1/2} \mathrm{e}^{-t/\beta^2} * c_1(t)\cos\theta, \tag{3.20a}$$

and the tangential component of the electric field

$$E_s(\theta, t) = \left[c_1(t) + \frac{2\alpha}{\beta^3}\left(\frac{t}{\pi}\right)^{1/2} \mathrm{e}^{-t/\beta^2} * c_1(t)\right]\sin\theta. \tag{3.20b}$$

Here $f * g$ denotes the conventional convolution integral between the functions f and g. For the temporal evolution of the charge concentration distribution within the EDL we similarly obtain

$$c(Y, \theta, t) = \frac{\alpha}{\beta}(\pi t)^{-1/2}\mathrm{e}^{-[t/\beta^2+(\beta Y)^2/(4t)]} * c_1(t)\cos\theta. \tag{3.21}$$

The foregoing results are presented in figure 1 describing the effects of α on the relaxation process for $\delta = 10^{-3}$. Part (a) shows the evolution of $\zeta^{(in)}(0, t)$, the induced

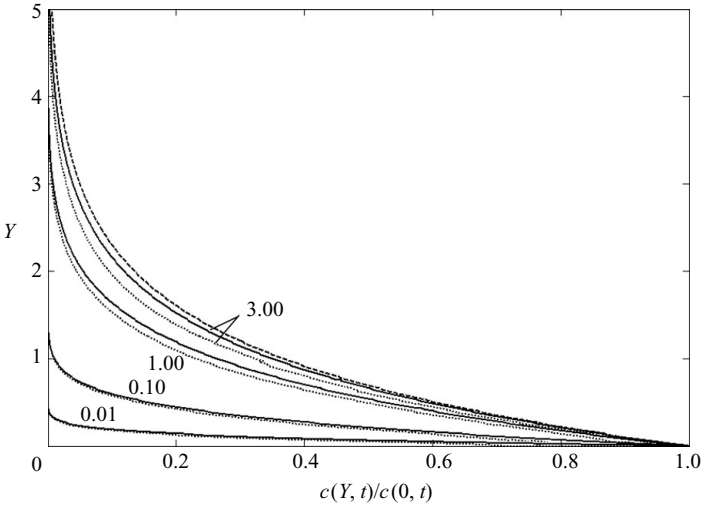

FIGURE 2. The effect of α on the relaxation to a Boltzmann distribution (dashed line) of $c(Y, 0, t)$ for $\delta = 10^{-3}$, $\alpha = 10^{-3}$ (solid curves) and $\alpha = 10^{2}$ (dotted curves).

zeta potential at $\theta = 0$, on a logarithmic scale of the dimensionless time (normalized by h^2/D) for the indicated values of α. The various curves appear qualitatively similar, starting initially from $\zeta^{(in)} = 0$ (in the absence of EDL) and approaching the common limit $\zeta^{(in)} = 1.5$. This specific invariance with α of the long-time limit, which results from the incorporation of the factor $\alpha/(1+\alpha)$ in the definition of ϕ_0, is unique to a spherical shape (see Yossifon *et al.* 2007). The main difference between the various curves appearing in figure 1 (*a*) is the time interval during which the evolution takes place. As stated before and in agreement with the above analysis, the relaxation time varies from the Debye scale ($\sim h^2/D$) for $\alpha \sim O(\delta)$ through the intermediate scale ($\sim ha/D$) for $\alpha \gtrsim 1$. Indeed, only minor quantitative differences appear when α is increased beyond $\alpha \approx 10$ or reduced below $\alpha \lesssim 10^{-3}$.

Part (*b*) of figure 1 similarly presents the relaxation to steady state of $E_s(\pi/2, t)$, the tangential component of the electric field at $\theta = \pi/2$. Whereas for the larger values of $\alpha \geqslant 1$, the time variation of E_s is similar to that of $\zeta^{(in)}$, for $\alpha \lesssim 0.1$. E_s possesses a non-zero initial value (at $t = 0^+$) which increases with diminishing α. For $\alpha \lesssim 10^{-4}$ E_s instantaneously relaxes (at $t = 0^+$) to the steady-state value ($E_s = 1.5$ for the present scaling). This observation is in agreement with the analytic solution for the potential φ_f satisfying a homogeneous Neumann condition on the surface of an insulating solid ($\alpha \to 0$) for all $t > 0$.

Figure 2 describes the temporal relaxation of $c(Y, 0, t)$, the electric charge density distribution within the diffuse EDL to the common equilibrium Boltzmann distribution (the dashed curve). Presented is the variation with the 'inner' variable Y of the ratio $c(Y, 0, t)/c(0, 0, t)$ (as obtained from (4.2) and (4.5)) for $\delta = 10^{-3}$ and $\alpha = 10^{-3}$ (solid lines) and $\alpha = 10^{2}$ (dotted lines) at the indicated values of t. While the curves pertaining to $\alpha = 10^{2}$ lag behind their respective counterparts for $\alpha = 10^{-3}$, the differences are relatively small. Furthermore, the various curves become indistinguishable from the Boltzmann distribution for all $t > 10$. Thus, in accordance with the above discussion (see (2.18) and (3.18) *et seq.*), the relaxation to the Boltzmann distribution takes place on the Debye time scale essentially irrespective of the specific value of α. From the union of Figures 1 and 2 we may therefore conclude that, for α

which is not very small (relative to unity), the relaxation process of the electrostatic problem consists of two phases: (i) the short-time establishment of a quasi-equilibrium Boltzmann charge distribution and (ii) the intermediate-time quasi-steady Ohmic charging of the EDL.

3.1.2. *The temporal evolution of the electro-osmotic flow*

By use of the relations (A.9) in conjunction with (3.8) and (3.9*a*) one gets

$$v_s^{(in)}(\theta, t) = \frac{2}{3} e_1(t) z_1(t) \sin\theta \cos\theta. \tag{3.22}$$

Hence, (A.10) and (A.11) imply that

$$\psi^{(in)}(R, \theta, t) = -\frac{2}{3} [e_1(t) z_1(t)] * L^{-1}\{S_2(R, t)\} \sin^2\theta \cos\theta, \tag{3.23}$$

in which $L^{-1}\{S_2(R, t)\}$ is given by (A.15) and both $e_1(t)$ and $z_1(t)$ are calculated from (3.7) by means of the results appearing in Appendix B. From (3.19) and (3.23) the velocity components of the 'induced' part of the flow can be obtained in a straightforward manner.

Figure 3 displays a comparison between the time evolution of the radial distribution of the azimuthal velocity component for $\delta = 10^{-3}$ and small (10^{-3}, part *a*) and large (10^2, part *b*) values of α, respectively. The solid curves present $v^{(in)}(R, \pi/4, t)$ at the indicated values of t. The dashed lines in both parts of the figure depict the steady distributions (which for spherical shapes are identical under the present scaling). The temporal evolution of the electro-osmotic flow is found to be governed by two processes: (i) the development of a fluid slip velocity at the wall and (ii) the diffusion of the vorticity generated there into the bulk solution. The latter effect is characterized in both cases by the same time scale (a^2/ν). Hence, the differences between parts (*a*) and (*b*) are to be rationalized in terms of the former mechanism which is related to the above-discussed relaxation processes of the electrostatic problem (respectively characterized by h^2/D for $\alpha \ll 1$ and ha/D for $\alpha \gtrsim 1$). Thus, in part (*a*) of the figure we observe that as early as $t = 1$ $v_s^{(in)}(\pi/4, t) = v^{(in)}(1, \pi/4, t) \gtrsim 0.2$ and that at $t = 10$ $v_s^{(in)}(\pi/4, t)$ has already attained its steady value. In contrast with these, in part (*b*) $v_s^{(in)}(\pi/4, t)$ is slowly increasing. For instance, at $t = 100$ $v_s^{(in)}(\pi/4, t)$ is still ≈ 0.08 and even at $t = 1000$ $v_s^{(in)}(t)$ has not yet reached its steady value. Since, for $\alpha \ll 1$ $v_s^{(in)}(\pi/4, t)$ is increasing at the wall much faster than the accompanying viscous diffusion of fluid motion into the bulk, steep velocity gradients appear near the sphere surface and persist through $t \approx 100$. In contrast, no such steep velocity gradients appear for the larger α, where both time scales characterizing the build up of $v_s^{(in)}(\pi/4, t)$ and vorticity diffusion, are comparable (i.e. $ha/D \approx a^2/\nu$). In agreement with this physical distinction, figure 3(*a*) clearly indicates a reversal in the direction of fluid motion with increasing radial distance, which could also be anticipated on grounds of continuity arguments and the quadrupolar symmetry of the problem (cf. (3.22)). This is expected to result in the appearance of closed-streamline patches adjacent to the sphere which, with increasing t will eventually diffuse into the bulk of the fluid with the streamlines gradually opening up. This phenomenon is indeed manifested in the streamline patterns obtained for $\gamma \to \infty$ in figure 4 (notwithstanding the larger intermediate value of $\alpha = 1$).

In most realistic micro-systems the equilibrium fixed surface charge σ and accompanying $\zeta^{(eq)}$ seldom vanish. Consequently, both contributions (3.9*a*, *b*) to the fluid slip velocity simultaneously exist and the resulting flow consists of both 'induced'

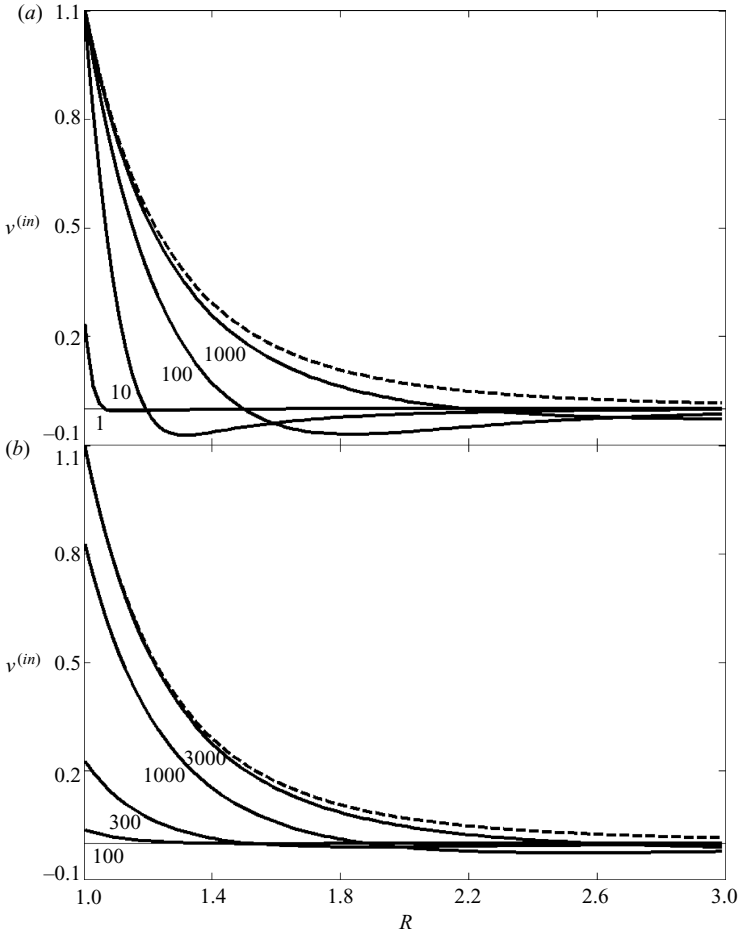

FIGURE 3. Time evolution of the function $v^{(in)}(R, \pi/4, t)$ characterizing the radial distribution of the azimuthal fluid velocity component for $\delta = 10^{-3}$, $\alpha = 10^{-3}$ (*a*) and 10^2 (*b*). The dashed lines mark the steady distribution.

(3.23) and 'equilibrium' parts as indicated in (A.1). From (3.7*b*), (3.9), (A.2) and (A.7) we obtain

$$\psi^{(eq)}(R, \theta, t) = \zeta^{(eq)} e_1(t) * L^{-1}\{S_1(R, t)\} \sin^2\theta, \tag{3.24}$$

where $L^{-1}\{S_1\}$ is given in (A.14). Unlike Morrison (1969), who assumed that E_s and hence $v_s^{(eq)}$ relaxed *instantaneously*, we consider here the detailed effects of the above-mentioned relaxation process of the electrostatic problem which shows up in (3.24) through the convolution with $e_1(t)$. Such effects appear to be important for sub-millisecond fast transient processes and should definitely be accounted for.

Figure 4 presents the time evolution of the resultant flow for $\delta = 10^{-3}$, $\alpha = 1$ and the indicated values of the parameter $\gamma = |\zeta^{(eq)}|^{-1}$ representing the relative magnitudes of the 'induced' and 'equilibrium' components ($\gamma = 0$ corresponding to $\psi^{(eq)}$ and $\gamma \to \infty$ to $\psi^{(in)}$, respectively). In agreement with the earlier discussion of the various time scales characterizing the intriguing relaxation process, we observe here that, by $t = 10^3$, and for all values of γ, none of the flows has yet reached the corresponding steady state. While each of the respective components of the flow pattern possesses fore–aft

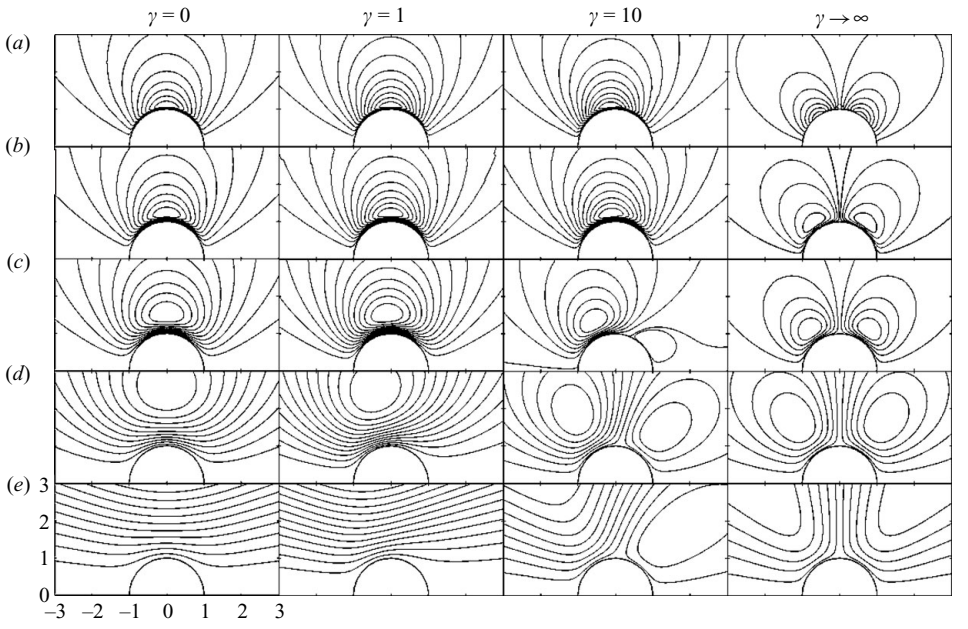

FIGURE 4. The temporal evolution of the streamline pattern for $\delta = 10^{-3}$ and $\alpha = 1$. Presented are the patterns at $t = 1$ (*a*), 10 (*b*), 100 (*c*), 1000 (*d*) and ∞ (*e*) for the indicated values of γ.

symmetry, it is anticipated that (similarly to the corresponding steady problem, cf. Squires & Bazant 2004) for all finite values of γ, the superposition of the 'induced' and 'equilibrium' parts will break this symmetry. However, for all values of $\gamma < \infty$ presented, the streamline patterns at the earlier instants of time $t = 1$, 10 are nearly identical to the corresponding 'equilibrium' pattern $\gamma = 0$ (all possessing the same dipolar fore–aft symmetry). This initial physical dominance of the 'equilibrium' part is related to its linear-dependence as opposed to the quadratic-dependence of the 'induced' part on the initially small values of E_s (see the curve $\alpha = 1$ in figure 1*b*). Indeed, for $\gamma = 1$ the streamline pattern remains nearly symmetric even as late as $t = 10^2$. At this time a flow stagnation point is apparent on the aft portion of the sphere for $\gamma = 10$ and the streamline pattern is clearly asymmetric.

4. Discussion and concluding remarks

We have studied the macro-scale description of the temporal evolution of electro-kinetic flows in the vicinity of polarizable solids following the application of a transient electric field. Towards this end we have derived the effective transient boundary conditions (2.15′) and (2.16′) directly connecting the electric potentials across the EDL (thus, eliminating the need to resolve its details). These newly derived conditions apply to general transient induced-charge electro-kinetic (i.e. electro-osmosis, electrophoresis, dipolophoresis, etc.) problems involving polarizable solids of arbitrary geometry and dielectric constants in the presence of general spatially non-uniform and time-dependent weak external electric fields.

The pair of conditions (2.15′) and (2.16′), respectively, replace the Robin-type (Yossifon *et al.* 2007) and homogeneous Neumann conditions pertaining to the corresponding steady problem and appropriately converge to them in the long time limit. The departure of (2.16′) from the homogeneous Neumann condition represents

the (primarily Ohmic) transient charging process of the EDL. Owing to this difference, the pair of electrostatic problems within the solid and the bulk electroneutral solution are coupled to each other and need to be resolved simultaneously (as opposed to the steady-state problem where these may be solved recursively).

Our analysis demonstrates that the time evolution of the electrostatic problem mainly involves two physical processes: (i) Ohmic charging of the EDL resulting from the combined effects of the transient external field and the polarization of the solid and (ii) charge transfer across the EDL to establish a quasi-steady equilibrium Boltzmann distribution. The latter, which is essentially a diffusive process, is characterized by the Debye time scale h^2/D irrespective of the value of the parameter α. The above analysis also demonstrates that the time scale of the former charging process is monotonically increasing with $\alpha \geqslant \delta$, ultimately becoming equal to the intermediate time scale ha/D for $\alpha \gtrsim 1$ (in agreement with common RC models). Thus, for the latter case, when considering practical transient electro-kinetic problems concerning micro-particles or microfluidic applications, the evolution of the electrostatic and hydrodynamic processes takes place on comparable time scales.

Identifying the parameter α as the ratio of the capacitance of the dielectric solid and that of the EDL provides a qualitative interpretation of our results in terms of an equivalent electric-circuit model. Furthermore, through this established correspondence, the present rigorous scheme substantiates earlier results regarding the effects of solid material dielectric properties on the time scale of the relaxation process, the induced zeta potential, etc.

It is worthwhile to note that $\alpha \approx 1$ practically means a large but *finite* value of the permittivities ratio $\varepsilon_w/\varepsilon_f$. While solids are often classified as ideally polarizable (conducting) or non-polarizable (insulating), the entire spectrum of properties may appear in natural or synthetic materials, including dielectrics possessing large relative permittivities (see, e.g. Arlt, Hennings & de With 1985; Kuo *et al.* 2004; Flores-Rodriguez & Markx 2006) satisfying $\alpha \gg \delta$.

The use of the newly proposed general macro-scale model has been illustrated by considering the transient induced-charge electro-osmosis around a dielectric sphere. The explicit results thus obtained demonstrate the qualitative physical differences in the time evolution of the induced fluid motion when the electrostatic relaxation process is either relatively fast (small α) or slow ($\alpha \gtrsim 1$). Since most realistic microfluidic and colloidal systems usually include an equilibrium fixed-charge contribution to the zeta potential, the electro-osmotic flow field may be calculated via a superposition of the respective 'induced' and 'equilibrium' contributions. Each of these transient components possesses the same geometrical symmetry as in the corresponding steady problem. Their superposition is thus expected to lead to symmetry-breaking phenomena by destroying the common fore–aft symmetry. A remarkable feature depicted in figure 4 is, however, that for $\alpha \approx 1$ and all $\gamma < \infty$, the initial flow streamline pattern is essentially dominated by the 'equilibrium' contribution associated with $\zeta^{(eq)}$ exhibiting the usual fore–aft symmetry. Furthermore, for $\gamma \leqslant 1$, this symmetry persists over a significant time interval (nearly through $t = 100$). This particular mode of time evolution physically demonstrates the role of the electrostatic relaxation process in the extended suppression of the 'induced' contribution to the flow field for $\alpha \gg \delta$. The endurance of the fore–aft symmetry reflects the early dominance of the 'equilibrium' contribution which is linear in (as opposed to the quadratic dependence of the 'induced' contribution upon) the initially small tangent electric field.

The transient induced-charge electro-osmosis problem around a dielectric spherical particle has been selected in this paper for two reasons: Firstly, a spherical shape is the

most common model for colloidal particles. The other reason is that, because of the perfect isotropy, the dielectric sphere is amenable to analytical analysis. Application of the newly established macro-scale description to problems involving other geometrical configurations of polarizable solids (e.g. the time evolution of the flow around a polarizable corner which is relevant to mixing processes, cf. Wang *et al.* 2006) or other transient induced-charge electro-kinetic phenomena (e.g. the dipolophoresis of a dielectric sphere in a transient non-uniform electric field) are currently under way and will be reported elsewhere. Furthermore, it is recalled that the present description has been developed within the framework of the common assumptions of a thin EDL and weak fields. The former assumption is safely satisfied (with the possible exception of certain singular points) in most micro-scale applications. However, from both practical and fundamental aspects, relaxing the latter restriction seems a useful future extension of the present work. Finally, it is desirable to examine the theoretical predictions of the present analysis through a direct comparison with experimental results. Obviously, the short sub-millisecond time scales involved get in the way of an experimental resolution of these rapid electro-kinetic transient phenomena. Nevertheless, the recent advances in the state-of-the-art μPIV techniques (e.g. Yan *et al.* 2007) indicate that such a direct comparison may be feasible in the near future.

I. Frankel acknowledges the support of the J. and J. Gringorten Aeronautical Research Fund and T. Miloh the partial support of the Lazarus Brothers Chair in Hydrodynamics.

Appendix A: Calculation of ψ

It is convenient to represent ψ via the superposition

$$\psi = \psi^{(in)} + \psi^{(eq)}, \tag{A 1}$$

where each part satisfies (3.16*b*) for the corresponding term on the right-hand side of (3.8).

(i) *The 'equilibrium' part* $\psi^{(eq)}$*:*

The functional form of (3.9*b*) together with the relation (3.14*b*) suggest

$$\psi^{(eq)}(R,\theta,t) = \sum_n \bar{\psi}_n^{(eq)}(R,t)\dot{P}_n(\mu)\sin^2\theta. \tag{A 2}$$

Substituting this expression in (3.15) while making use of the Legendre equation satisfied by $P_n(\mu)$ and the orthogonality property (A 8), we see that each $\bar{\psi}_n^{(eq)}(R,t)$ needs to satisfy

$$\left[\frac{\partial^2}{\partial R^2} - \frac{n(n+1)}{R^2}\right]\left[\frac{\partial^2}{\partial R^2} - \frac{n(n+1)}{R^2} - \frac{\partial}{\partial t}\right]\bar{\psi}_n^{(eq)}(R,t) = 0. \tag{A 3}$$

Laplace transforming (A 3) and (3.16) while utilizing the homogeneous initial condition we obtain the equation

$$\left[\frac{\partial^2}{\partial R^2} - \frac{n(n+1)}{R^2}\right]\left[\frac{\partial^2}{\partial R^2} - \frac{n(n+1)}{R^2} - s\right]S_n(R,s) = 0, \tag{A 4}$$

and boundary conditions

$$S_n = 0 \quad \text{and} \quad \frac{\mathrm{d}S_n}{\mathrm{d}R} = 1 \quad \text{at} \quad R = 1, \tag{A 5a,b}$$

where $L\left\{\bar{\psi}_n^{(eq)}\right\} = \zeta^{(eq)} L\left\{e_n(t)\right\} S_n(R, s)$. From (A 4) we obtain the solution

$$S_n(R, s) = A_n(s)R^{-n} + B_n(s)R^{n+1}\left(\frac{1}{R}\frac{\mathrm{d}}{\mathrm{d}R}\right)^{n+1} \mathrm{e}^{-\sqrt{s}R} \tag{A 6}$$

which appropriately attenuates as $R \to \infty$. The coefficients $A_n(s)$ and $B_n(s)$ are to be determined via application of (A 5). Once this is accomplished solution (A 2) is calculated through

$$\bar{\psi}_n^{(eq)}(R, t) = \zeta^{(eq)} e_n(t) * L^{-1}\left\{S_n(R, s)\right\}. \tag{A 7}$$

(ii) *The 'induced' part* $\psi^{(in)}$*:*

Making use of the orthogonality property

$$\int_{-1}^{1} (1-\mu^2)\dot{P}_k(\mu)\dot{P}_l(\mu)\,\mathrm{d}\mu = \frac{2l(l+1)}{2l+1}\delta_{kl}, \tag{A 8}$$

we expand

$$P_n(\mu)\dot{P}_m(\mu) = \sum_l q_l \dot{P}_l(\mu), \tag{A 9a}$$

where

$$q_l = \frac{2l+1}{2l(l+1)} \int_{-1}^{1} (1-\mu^2) P_n(\mu)\dot{P}_m(\mu)\dot{P}_l(\mu)\,\mathrm{d}\mu, \tag{A 9b}$$

to write (3.9*a*)

$$v_s^{(in)} = \sum_{m,n} e_m(t) z_n(t) \sum_l q_l\, \dot{P}_l(\mu)\sin\theta, \tag{A 9c}$$

which, similarly to (A 2), suggests the solution

$$\psi^{(in)} = \sum_{l,m,n} \psi_{lmn}^{(in)}(R, t)\dot{P}_l(\mu)\sin^2\theta. \tag{A 10}$$

Following the same route as (A 3)–(A 7) we eventually obtain

$$\psi_{lmn}^{(in)} = q_l[e_m(t)z_n(t)] * L^{-1}\left\{S_l(R, s)\right\}. \tag{A 11}$$

For $n = 1, 2$ we obtain from (A 5) and (A 6)

$$S_1 = \left(\frac{1}{\sqrt{s}} + \frac{1}{s}\right)\frac{1}{R} - \left(\frac{1}{\sqrt{s}} + \frac{1}{Rs}\right)\mathrm{e}^{-\sqrt{s}(R-1)} \tag{A 12}$$

and

$$S_2 = \frac{1}{s^2 + s^{3/2}}\left[\left(3s^{1/2} + 3s + s^{3/2}\right)\frac{1}{R^2} - \left(\frac{3\sqrt{s}}{R^2} + \frac{3s}{R} + s^{3/2}\right)\mathrm{e}^{-\sqrt{s}(R-1)}\right]. \tag{A 13}$$

These are readily inverted to yield

$$L^{-1}\{S_1\} = \frac{1}{R}\left[1 + (\pi t)^{-1/2}\right] - (\pi t)^{-1/2}\,\mathrm{e}^{-(R-1)^2/(4t)} - \frac{1}{R}\mathit{erfc}\left(\frac{R-1}{2t^{1/2}}\right) \tag{A 14}$$

and

$$L^{-1}\{S_2\} = \left[3+(\pi t)^{-1/2}-\mathrm{e}^{t}erfc\left(t^{1/2}\right)\right]\frac{1}{R^2}-(\pi t)^{-1/2}\mathrm{e}^{-(R-1)^2/(4t)}-\frac{3}{R^2}erfc\left(\frac{R-1}{2t^{1/2}}\right) + \left(1-\frac{3}{R}+\frac{3}{R^2}\right)\mathrm{e}^{R-1+t}erfc\left(\frac{R-1}{2t^{1/2}}+t^{1/2}\right), \quad (A\,15)$$

respectively.

Appendix B: Calculation of $c_1(t)$

Representing

$$C_1(s) = -\left(\frac{E_0 a}{\phi_0}\right)\frac{3}{(2+\alpha/\delta)}\frac{1}{s}\left(1+\frac{\alpha}{\delta}\frac{\lambda}{\Delta}-2\frac{\alpha}{\Delta}\right), \quad (B\,1)$$

where $\Delta = (2+\alpha/\delta)\lambda^3 - (\alpha/\delta)\lambda + 2\alpha$, we first focus on the inverse transform $L^{-1}\{(s\Delta)^{-1}\}$. It is useful to note that for all practical cases $\varepsilon_w/\varepsilon_f \gtrsim 0.05$ (e.g. Takhistov *et al.* 2003, for acrylic and an aqueous solution). We therefore assume throughout the subsequent derivation that $\delta^2 \ll \min\{1, \varepsilon_w/\varepsilon_f\}$. Under this assumption, the cubic $\Delta(\lambda)$ possesses three simple real zeros

$$\lambda_1 \sim 2\delta, \quad \text{and} \quad \lambda_{2,3} \sim \pm\left(\frac{\alpha}{\alpha+2\delta}\right)^{1/2} - \delta. \quad (B\,2)$$

By the above selection of the branch $\lambda > 0$ for $s > 0$, only λ_1 and λ_2 are relevant to the problem at hand. The singularities of $(s\Delta)^{-1}$ thus consist of the simple poles at

$$s_0 = 0, \quad s_1 \sim -1/\beta^2, \quad s_2 \sim -\frac{2\delta}{\beta^2}\left[\frac{1}{\alpha+2\delta}+\left(\frac{\alpha}{\alpha+2\delta}\right)^{1/2}\right]$$

and the branch cut extending from $s = -1/\beta^2$ to infinity along the negative real axis. Summation of the residues at the poles and the contribution of the branch cut yields

$$L^{-1}\left\{\frac{1}{s\Delta}\right\} \sim \frac{1}{2(1+\alpha)} + 4\frac{\delta^2}{\alpha}\mathrm{e}^{s_1 t} - \frac{\delta}{\alpha}\frac{s_1}{s_2}\left(\frac{\alpha}{\alpha+2\delta}\right)^{1/2}\mathrm{e}^{s_2 t} + \frac{1}{\pi}\int_0^\infty K(\xi,t)\left[\left(2+\frac{\alpha}{\delta}\right)\xi+\frac{\alpha}{\delta}\right]\mathrm{d}\xi, \quad (B\,3)$$

wherein we define

$$K(\xi,t) = \frac{(1+\xi)^{-1}\xi^{1/2}\,\mathrm{e}^{(1+\xi)s_1 t}}{(2+\alpha/\delta)^2\,\xi^3 + 2\,(2+\alpha/\delta)\,(\alpha/\delta)\xi^2 + (\alpha/\delta)^2\,\xi + 4\alpha^2}.$$

Similarly we obtain

$$L^{-1}\left\{\frac{\lambda}{s\Delta}\right\} \sim \left\{\frac{1}{2(1+\alpha)} + 8\frac{\delta^3}{\alpha}\,\mathrm{e}^{s_1 t} - \frac{s_1}{s_2}\left(\frac{\delta}{\alpha+2\delta}\right)\mathrm{e}^{s_2 t} + \frac{2\alpha}{\pi}\int_0^\infty K(\xi,t)\,\mathrm{d}\xi\right\}. \quad (B\,4)$$

Combining these results and (B 1) we finally obtain

$$c_1(t) \sim -\left(\frac{E_0 a}{\phi_0}\right)\left\{\left(\frac{6\delta^2}{\alpha+2\delta}\right)\frac{s_1}{s_2}\left[-\frac{1}{2\delta}\left(\frac{\alpha}{\alpha+2\delta}\right)+\left(\frac{\alpha}{\alpha+2\delta}\right)^{1/2}\right]\mathrm{e}^{s_2 t} + \frac{3}{2(1+\alpha)} - \frac{6\alpha}{\pi}\int_0^\infty K(\xi,t)\xi\,\mathrm{d}\xi.\right\} \quad (B\,5)$$

Similarly to the above $C_1(s)$, application of (2.15) and (2.16) yields $B_1(s) = L\{b_1(t)\}$, one thereby gets

$$B_1(s) = -\left(\frac{E_0 a}{\phi_0}\right)\frac{1}{s}\left[\frac{1-\alpha/\delta}{2+\alpha/\delta} + \frac{3\alpha}{\delta}\left(\frac{\lambda}{\Delta}+\frac{\alpha}{\Delta}\right)\right]. \tag{B 6}$$

The inverse transform is calculated by making use of (B 3) and (B 4) to yield $b_1(t)$. In the limit when both δ and $1/\alpha \to 0$ one gets φ_f (3.19″).

REFERENCES

Ajdari, A. 2000 Pumping liquids using asymmetric electrode arrays. *Phys. Rev.* E **61**, 45–48.

Arlt, G., Hennings, D. & de With, G. 1985 Dielectric properties of fine-grained barium titanate ceramics. *J. Appl. Phys.* **58**, 1619–1625.

Bazant, M. Z. & Squires, T. M. 2004 Induced-charge electro-kinetic phenomena: theory and microfluidic applications. *Phys. Rev. Lett.* **92**, 066101-1-4.

Bazant, M. Z., Thornton, K. & Ajdari, A. 2004 Diffuse-charge dynamics in electrochemical systems. *Phys. Rev.* E **70**, 021506–24.

Brown, A. B. D., Smith, C. G. & Rennie, A. R. 2002 Pumping of water with AC electricfields applied to asymmetric pairs of microelectrodes. *Phys. Rev.* E **63**, 016305–8.

Campisi, M., Accoto, D. & Dario, P. 2005 AC electroosmosis in rectangular microchannels. *J. Chem. Phys.* **123**, 204724–9.

Chu, K. T. & Bazant, M. Z. 2006 Nonlinear electrochemical relaxation around conductors. *Phys. Rev.* E **74**, 011501–25.

Dose, E. V. & Guiochon, G. 1993 Timescales of transient processes in capillary electrophoresis. *J. Chromatogr.* A **652**, 263–275.

Dukhin, A. S. 1986 Pair interaction of disperse particles in electric-field. 3. Hydrodynamic interaction of ideally polarizable metal particles and dead biological cells. *Colloid J. USSR* **48**, 376–381.

Dukhin, A. S. & Murtsovkin, V. A. 1986 Pair interaction of particles in electric-field. 2. Influence of polarization of double-layer of dielectric particles on their hydrodynamic interaction in a stationary electric-field. *Colloid J. USSR* **48**, 203–209.

Erickson, D. & Li, D. 2003 Analysis of alternating current electroosmotic flows in a rectangular microchannel. *Langmuir* **19**, 5421–5430.

Fan, Z. H. & Harrison, D. J. 1994 Micromachining of capillary electrophoresis injectors and separators on glass chips and evaluation of flow at capillary intersections. *Anal. Chem.* **66**, 177–184

Flores-Rodriguez, N. F. & Markx, G. H. 2006 Anomalous dielectrophoretic behaviour of barium titanate microparticles in concentrated solutions of ampholytes. *J. Phys.* D **39**, 3356–3361.

Gamayunov, N. I., Murtsovkin, V. A. & Dukhin, A. S. 1986 Pair interaction of particles in electric-field. 1. Features of hydrodynamic interaction of polarized particles. *Colloid J. USSR* **48**, 197–203.

Gonzalez, A., Ramos, A., Green, N. G., Castellanos, A. & Morgan, H. 2000 Fluid flow induced by nonuniform AC electric fields in electrolytes on microelectrodes. II. A linear double-layer analysis. *Phys. Rev.* E **61**, 4019–4028.

Hanna, W. T. & Osterle, J. F. 1968 Transient electro-osmosis in capillary tubes. *J. Chem. Phys.* **49**, 4062–4068.

Happel, J. & Brenner, H. 1965 *Low Reynolds Number Hydrodynamics*. Prentice-Hall.

Harnett, C. K., Templeton, J., Dunphy-Guzman, K. A., Senousya, Y. M. & Kanouff, M. P. 2008 Model based design of a microfluidic mixer driven by induced charge electroosmosis. *Lab Chip.* **8**, 565–572.

Ivory, C. F. 1983 Transient electroosmosis: the momentum transfer coefficient. *J. Colloid Interface Sci.* **96**, 296–298.

Ivory, C. F. 1984 Transient electrophoresis of a dielectric sphere. *J. Colloid Interface Sci.* **100**, 239–249.

Jacobson, S. C., Culbertson, C. T., Daler, J. E. & Ramsey, J. M. 1998 Microchip structures for submillisecond electrophoresis. *Anal. Chem.* **70**, 3476–3480.

Jacobson, S. C., Hergenroder, R., Koutny, L. B. & Ramsey, J. M. 1994 High-speed separations on a microchip. *Anal. Chem.* **66**, 1114–1118.

Kang, Y., Yang, C. & Huang, X. 2002 Dynamic aspects of electroosmotic flow in a cylindrical Microcapillary. *Int. J. Engng Sci.* **40**, 2203–2221.

Keh, H. J. & Huang, Y. C. 2005 Transient electrophoresis of dielectric spheres. *J. Colloid Interface Sci.* **291**, 282–291.

Keh, H. J. & Tseng, H. C. 2001 Transient electro-kinetic flow in fine capillaries. *J. Colloid Interface Sci.* **242**, 450–459.

Kuo, D. H., Chang, C. C., Su, T. Y., Wang, W. K. & Lin, B. Y. 2004 Dielectric properties of three ceramic/epoxy composites. *Mater. Chem. Phys.* **85**, 201–206.

Levich, V. G. 1962 *Physicochemical Hydrodynamics*. Prentice-Hall.

Lide, D. R. 1994 *CRC Handbook of Chemistry and Physics*, 74th ed. CRC Press.

Luo, W. J. 2004 Transient electroosmotic flow induced by DC or AC electric fields in a curved microtube. *J. Colloid Interface Sci.* **278**, 497–507.

Lyklema, J. 1995 *Fundamentals of Interface and Colloid Science*. Vol. II. Solid–liquid Interfaces. Academic Press.

Macdonald, J. R. 1970 Double layer capacitance and relaxation in electrolytes and solids. *Trans. Faraday Soc.* **66**, 943–958.

Miloh, T. 2008*a* Dipolophoresis of nanoparticles. *Phys. Fluids* **20**, 063303–12.

Miloh, T. 2008*b* A unified theory for dipolophoresis of nanoparticles. *Phys. Fluids.* **20**, 107105–14.

Mishchuk, N. A. & Gonzalez, C. F. 2006 Nonstationary electroosmotic flow in open cylindrical capillaries. *Electrophoresis* **27**, 650–660.

Morrison, F. A. 1969 Transient electrophoresis of a dielectric sphere. *J. Colloid Interface Sci.* **29**, 687–691.

Morrison, F. A. 1971 Transient electrophoresis of an arbitrarily oriented cylinder. *J. Colloid Interface Sci.* **36**, 139–143.

Murtsovkin, V. A. 1996 Nonlinear flows near polarized disperse particles. *Colloid J.* **58**, 341–349.

Nadal, F., Argoul, F., Kestener, P., Pouligny, B., Ybert, C. & Ajdari, A. 2002 Electrically induced flows in the vicinity of a dielectric stripe on a conducting plane. *Eur. Phys. J.* E **9**, 387–399.

Ramos, A., Morgan, H., Green, N. G. & Castellanos, A. 1999 AC electric-field- induced fluid flow in microelectrodes. *J. Colloid Interface Sci.* **217**, 420–422.

Santiago, J. G. 2001 Electroosmotic flows in microchannels with finite inertial and pressure forces. *Anal. Chem.* **73**, 2353–2365.

Simonov, I. N. & Dukhin, S. S. 1973 Theory of electrophoresis of solid conducting particles in case of ideal polarization of a thin diffuse double-layer. *Colloid J.* **35**, 173–176.

Simonov, I. N. & Shilov, V. N. 1973 Theory of the polarization of the diffuse part of a thin double layer at conducting, spherical particles in an alternating electric field. *Colloid J.* **35**, 350–353.

Soderman, O. & Jonsson, B. 1996 Electro-osmosis: velocity profiles in different geometries with both temporal and spatial resolution. *J. Chem. Phys.* **105**, 10300–10311.

Squires, T. M. & Bazant, M. Z. 2004 Induced-charge electro-osmosis. *J. Fluid Mech.* **509**, 217–252.

Takhistov, P., Duginova, K. & Chang, H. C. 2003 Electro-Kinetic mixing due to electrolyte depletion at microchannel junction. *J. Colloid Interface Sci.* **263**, 133–143.

Thamida, S. K. & Chang, H. C. 2002 Nonlinear electro-kinetic ejection and entrainment due to polarization at nearly insulated wedges. *Phys. Fluids.* **14**, 4315–4328.

Wang, S. C., Chena, H. P., Lee, C. Y., Yu, C. C., & Chang, H. C. 2006 AC electro- osmotic mixing induced by non-contact external electrodes. *Biosens. Bioelectr.* **22**, 563–567.

Yan, D., Yang, C., Nguyen, N. T. & Huang, X. 2007 Diagnosis of transient electro-kinetic flow in microfluidic channels. *Phys. Fluids* **19**, 017114–10.

Yang, C., Ng, C. B. & Chan, V. 2002 Transient analysis of electroosmotic flow in a slit microchannel. *J. Colloid Interface Sci.* **248**, 524–527.

Yang, M. C., Ooi, K. T., Wong, T. N. & Masliyah, J. H. 2004 Frequency dependent laminar electroosmotic flow in a closed - end rectangular microchannel. *J. Colloid Interface Sci.* **275**, 679–698.

Yariv, E. 2008 Slender-body approximations for electro-phoresis and electro-rotation of polarizable particles. *J. Fluid Mech.* **613**, 85–94.

Yossifon, G., Frankel, I. & Miloh, T. 2006 On electro-osmotic flows through micro channel junctions. *Phys. Fluids.* **18**, 117108–9.

Yossifon, G., Frankel, I. & Miloh, T. 2007 Symmetry breaking in induced-charge electroosmosis over polarizable spheroids. *Phys. Fluids* **19**, 068105–4.

Zhang, Y., Wong, T. N., Yang, C. & Ooi, K. T. 2006 Dynamic aspects of electroosmotic flow. *Microfluid Nanofluid* **2**, 205–214.